

# Natural Polarization Modes in Pulsar Magnetospheres

A. von Hoensbroech<sup>1,2</sup>, H. Lesch<sup>2</sup> and T. Kunzl<sup>2,3</sup>

<sup>1</sup> Max-Planck-Institut für Radioastronomie, Auf dem Hügel 69, D-53121 Bonn, Germany.

<sup>2</sup> Institut für Astronomie und Astrophysik der Universität München, Scheinerstr. 1, D-81679 München, Germany.

<sup>3</sup> Max-Planck-Institut für extraterrestrische Physik, Giessenbachstr., D-85740 Garching, Germany.

Received 9. March 1998 / Accepted 28. April 1998

**Abstract.** We present a comprehensive investigation of the radio polarization properties within the theory of natural electromagnetic wave modes in pulsar magnetospheres. Taking into account the curvature of the field lines, aberration effects and magnetic sweep-back we use the relativistic dielectric tensor in the low-density cold plasma approximation and derive the following polarization characteristics, which are in full agreement with the observational findings. Specifically, we demonstrate that **1.** The degree of linear polarization decreases with increasing frequency. **2.** The degree of circular polarization increases with increasing frequency. **3.** At high frequencies ( $\geq$  a few GHz) the degree of linear polarization is correlated to the spin down luminosity  $\dot{E}$ . **4.** At high frequencies long-period pulsars exhibit weaker linear polarization than their short-period counterparts. **5.** The difference between the refractive indices of the two natural wave modes decreases with increasing frequency which possibly results into a depolarization via superposition.

---

**Key words:** Plasmas; Polarization; Radiative transfer; Waves; Pulsars: general

## 1. Introduction

The polarization properties of pulsar radio emission are highly diverse. Nearly all possible polarization states have been detected, from pulsar to pulsar, from frequency to frequency, from pulse to pulse and even within one pulse profile. Nevertheless, some general statements can be made from an observational point-of-view, which must be explained by any plausible theoretical model:

- Pulsar radio emission is usually highly linearly polarized at low frequencies (in the following “low frequencies” defines frequencies up to about one GHz,

“high frequencies” corresponds to everything well above one GHz). Towards higher frequencies the radiation tends to depolarize (e.g. Manchester 1971, Xilouris et al. 1996).

- The observed polarization position angle (hereafter PPA) is a very stable feature which usually does not depend strongly on frequency. Apart from the occurrence of sudden  $\sim 90^\circ$  jumps, the so-called orthogonal polarization modes (hereafter OPM), the PPA usually follows a characteristic S-shaped curve. This curve can well be modelled by the rotating vector model (hereafter RVM) as proposed by Radhakrishnan & Cooke (1969). It is therefore thought to reflect the geometry of the radiating field lines.
- The sum of many (typically at least a few hundred) single pulses usually converges towards a characteristic average profile. In contrast, the individual pulses show a high variability. One well known single pulse feature is the *quasi-periodic microsecond-structure* (e.g. Cordes & Hankins 1977, Lange et al. 1998) observed over a broad frequency interval with no obvious frequency dependence of the quasi-periodicity. It is usually highly linearly and circularly polarized with a roughly constant PPA and often OPMs at the edges. This suggests that, during one micro-pulse, only one of the orthogonal polarization modes is observed. Another feature are the *subpulses*, sometimes drifting in pulse phase from one pulse to the next one. The PPA usually shows a swing during one subpulse, with the swing being stable relative to the subpulse. So when the subpulse drifts, the swing drifts as well, causing a depolarization in the integrated profile (e.g. Manchester et al. 1975).
- In average profiles and in individual pulses OPMs can be observed (e.g. Stinebring et al. 1984, Gangadhara 1997). The magnitude of these jumps is usually  $90^\circ$  but can also be less sometimes. Sudden orthogonal jumps in the PPA can be found in nearly all pulse phases and even at the same pulse phase in successive single pulses. The OPMs often coincide with changes in

---

Send offprint requests to: A. von Hoensbroech (avh@mpifr-bonn.mpg.de)

the handedness of the circular polarization. Their existence therefore suggests that the radiation preferentially takes two orthogonal elliptical states.

- Some pulsars show a high degree of circular polarization, preferentially near the centroid of the profile. Sometimes it also sometimes shows a sense reversal near the centroid (Radhakrishnan & Rankin 1990). Recent observations show that a few pulsars have a strong increase in their degree of circular polarization towards high frequencies together with a decrease in linear polarization, thus suggesting that a process might be active which transforms linear into circular polarization (von Hoensbroech et al. 1998).
- At low frequencies there seems to be no significant relation between the average degree of polarization and any other pulsar parameter. At higher frequencies, however, correlations have been found between the degree of polarization and the spin down luminosity  $\dot{E}$  respectively the surface acceleration potential (Morris et al. 1981, Xilouris et al. 1995 and von Hoensbroech et al. 1998). Pulsars with a high  $\dot{E}$  (respectively a short period and a large period derivative) show a higher average polarization at high frequencies than those with a lower  $\dot{E}$ . This suggests that for these pulsars a possible depolarization process becomes important at higher frequencies than for the other pulsars. Closely connected to this is an anti-correlation between the degree of polarization at high frequencies and the period. Only rapidly rotating pulsars seem to have highly polarized radio emission (von Hoensbroech et al. 1998).
- Several authors estimated the emission altitudes where the observed radiation is produced and studied if there is a frequency dependence of this altitude (Cordes 1978, Rankin 1990, Thorsett 1991, Blaskiewicz et al. 1991, Gil 1991, Phillips 1992, Gil & Kijak 1997, von Hoensbroech & Xilouris 1997, Kramer et al. 1997). Various independent methods were used and all authors came to the conclusion that the radio emission originates from a region close to the pulsar surface at a few percent of the light cylinder radius (at least for “normal” – non millisecond – pulsars). The frequency dependence of the emission height is thought to be small, if it exists at all.

All these observational facts have to be explained within a general model for the polarization of pulsar radio emission. Basically, there are two aspects which must be considered. One is the polarization characteristic of the emission process itself, and the other one is the influence of the magnetosphere on the propagating radiation. In this paper we concentrate on the possible role of propagation for the polarization because this can be considered independently of the possible radiation mechanisms.

The magnetosphere of a pulsar is filled with a plasma which is streaming relativistically outwards along the open

field lines. A number of articles has already been published on propagational effects in this plasma.

Cocke & Pacholczyk (1976) considered the effect of Faraday pulsation for quasi-transverse propagation. Faraday pulsation is the general case of Faraday rotation. It occurs when a polarized beam decays into two elliptical orthogonal modes which propagate with different phase velocities. The PPA of the resulting beam gets rotated and the polarization changes between linear and circular. In a series of papers Melrose & Stoneham (1977), Melrose (1979) and Allen & Melrose (1982) derived an approximation for the dispersion tensor and calculated the properties of the natural wave modes in the plasma (see also Lyutikov 1998). They assumed that the polarization of the propagating electromagnetic wave follows the shape of the natural wave modes up to a certain radius of limiting polarization (hereafter  $R_{LP}$ ). The radiation then escapes with the polarization properties of the natural wave modes at  $R_{LP}$ . Barnard (1986) places  $R_{LP}$  at the place of cyclotron resonance. For normal pulsars this resonance occurs at a few 10% of the light cylinder radius, but for short period pulsars ( $P \leq 0.06s$ ) this resonance is outside  $R_{LC}$ .

Cheng & Ruderman (1979) considered adiabatic walking to be responsible for the variable polarization in subpulses. The polarization properties were derived for different emission mechanisms and plasma compositions.

Harding & Tadamaru (1979, 1980, 1981) presented numerical calculations on the propagation of linearly polarized pulses through a shearing plasma. They show that this can account for micro-structure, circular polarization and rotation of the PPA.

Barnard & Arons (1986) and Arons & Barnard (1986) have calculated the dispersion relations for the X- and the O-mode in an ultra-relativistic, one-dimensional plasma for distribution functions in  $e^-$  and  $e^+$  (the O-mode has its electric field vector in the plane of curvature of the magnetic field, the X-mode perpendicular to it). The X-mode is purely linearly polarized and propagates easily through the magnetosphere whereas the O-mode can have some circular contributions and follows the bending of the field lines. This causes a separation of the OPs (McKinnon 1997).

Calculations concerning the propagation characteristics of the various natural modes have also been presented by Beskin et al. (1993). Using the limit of infinite magnetic field strength they conclude that only the electromagnetic X-mode can propagate freely through the magnetosphere. The angular dependence of the properties of the modes and the influence of the cyclotron resonance are derived. This resonance becomes only significant, if the secondary particle production rate is high ( $\geq 10^4$  per primary particle) thus leading to a much higher plasma density. The different mode properties also account for the circular polarization often observed in core components.

In this paper we extended the ideas proposed by Melrose & Stoneham(1977), Melrose (1979) and Allen & Melrose (1982). We derive the properties of the natural wave modes throughout the magnetosphere with special respect to the angle between the propagating wave and the magnetic field. We make predictions for the qualitative dependence of the polarimetric properties with frequency and various pulsar parameters. These predictions are then compared with the observations.

## 2. Method

### 2.1. Global picture

For our calculations we use the following global picture for the pulsar radio emission (e.g. Manchester & Taylor 1977): The neutron star (hereafter NS) has a strong dipolar magnetic field which produces a corotating magnetosphere filled with charged particles which are drawn from the NS surface. It is convenient to define the light cylinder radius  $R_{LC}$  of the magnetosphere at which the corotation velocity is equal to the speed of light

$$R_{LC} = \frac{cP}{2\pi}, \quad (1)$$

where  $c$  is the speed of light and  $P$  is the rotation period of the NS. Those field lines which do not close within  $R_{LC}$  define the polar cap. The angular size of the polar cap is therefore given by

$$\phi_{lof} = \arcsin \left( \sqrt{\frac{R_{NS}}{R_{LC}}} \right) \quad (2)$$

with  $R_{NS}$  being the neutron star radius ( $R_{NS} = 10$  km, lof stands for **l**ast **o**pen **f**ield line). The particles get accelerated above the polar cap and flow relativistically outwards along the open field lines. The motion is one dimensional (all particles are in their lowest Landau-levels). Only one type of particles is considered (here electrons). Some pair producing processes might be active, thus adding another type of particles but we assume that there will always be one type dominating. The problems of strong pair production follows from considerations by Kunzl et al. which will be presented in a forthcoming paper.

According to the model of Goldreich & Julian (1969) we use the following density:

$$n_{GJ} = \frac{4\pi\epsilon_0}{e} \cdot \frac{B_0}{P} \quad (3)$$

with  $e$  being the elementary charge and  $\epsilon_0 = 8.85 \cdot 10^{-12} \text{AsV}^{-1}\text{m}^{-1}$  the electric field constant. The surface magnetic field is defined as

$$B_0 = \sqrt{\frac{3c^3\mu_0 I}{32\pi^3 R_{NS}^6 \sin^2 \alpha}} \cdot P\dot{P}. \quad (4)$$

Here  $I = 10^{38} \text{kg} \cdot \text{m}^2$  is the moment of inertia of the NS and  $\alpha$  is the angle between the axis of rotation and the magnetic field axis.  $\dot{P}$  is the temporal derivative of the period,  $\mu_0 = 4\pi \cdot 10^{-7} \text{VsA}^{-1}\text{m}^{-1}$  the magnetic field constant. As the field is dipolar, the magnetic field strength and the local plasma density decrease with the cube of the distance from the NS.

At a few percent of  $R_{LC}$  the plasma produces radio emission. Since we want to make our calculations independent of the actual emission mechanism, we only assume that the particles initially have a certain Lorentz factor  $\gamma_{\text{beam}}$ , just before they radiate. The angle of emission is approximately  $1/\gamma_{\text{beam}}$  with respect to the field line along which they stream. After having radiated the particles flow further outwards and form the *background* plasma (bg) through which the radio waves have to propagate. Naturally the background plasma has a lower Lorentz factor than the radiating beam, i.e.  $\gamma_{\text{bg}} \ll \gamma_{\text{beam}}$ . Since the radio emission mechanism must be coherent and therefore very efficient, we assume that the energy spread of the background plasma is negligible above the emission region, thus the plasma is cold. In this case the cold plasma approximation applies and the energy distribution function is

$$f(\gamma) \simeq \delta(\gamma - \gamma_{\text{bg}}). \quad (5)$$

Further, we assume that we observe only one natural wave mode at a time. The polarization properties of the wave correspond to the local form of the natural wave modes up to  $R_{LP}$ . Above this radius, the interaction between the propagating wave and the plasma becomes so weak that the escaping wave preserves the state of polarization of that radius to infinity (see e.g. Melrose 1979, Barnard 1986 and Beskin et al. 1993). The maximum value for  $R_{LP}$  is  $R_{LC}$  but for most pulsars  $R_{LP}$  is probably reached at a closer distance. The minimum value for  $R_{LP}$  is the emission height itself.

The assumption that only one polarization mode is observed at a time might not always be true, but the existence of highly polarized OPMs indicates that this is at least sometimes true. If both modes are observed simultaneously the radiation gets depolarized. The results of the following discussion can therefore be regarded as upper limits for the observed degrees of polarization.

### 2.2. Geometrical Aspects

It is very important to analyze carefully the angle of the propagating wave relative to the magnetic field. This can be understood by an inspection of the extreme cases for parallel and transverse propagation. For an electromagnetic wave propagating parallel to a magnetic field, the natural wave modes are circular (R- and L-mode), whereas for transverse propagation they are linear (X- and O-mode) (see e.g. Krall & Trivelpiece 1986 or any standard

plasma physics book). For oblique propagation intermediate states appear (see Fig. 5). It is our aim to calculate these states as a function of the various parameters involved.

To derive the angle between the propagating wave and the magnetic field lines the following contributions have to be considered: The angle which originates from the dipolar structure of the field, the angle associated with the *aberration* and the degree of *magnetic sweep back*. Aberration is the apparent forward bending of the field lines through the rotation of the pulsar (Phillips 1992). The magnetic sweep back is caused by the magnetic dipole radiation. The magnetic field lines are bent in the direction opposite to the pulsar rotation by the electromagnetic torque of the neutron star (Shitov 1983).

We do not consider the relativistic beaming angle ( $\theta_{\text{beaming}} = 1/\gamma_{\text{beam}}$ ) outside the emitting region itself because this angle is symmetrical with respect to the direction of emission and will be averaged out statistically.

### 2.2.1. Dipolar contribution

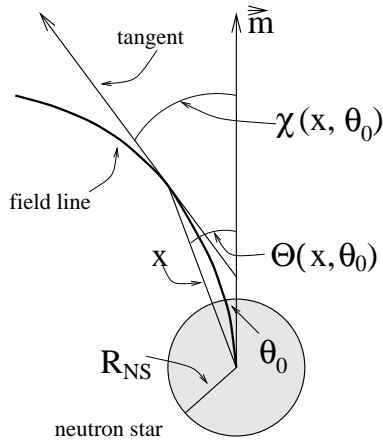


**Fig. 1.** Geometry to derive the tangential inclination  $\chi(x, \theta_0)$  of any dipolar field line with the footpoint-angle  $\theta_0$  at the radial distance  $x$ .

In a polar coordinate system, the quotient  $\sin^2 \theta / r$  is constant for a dipolar field line. Having the NS in the centre, and defining each field line by its *footpoint* (point of intersection) at the NS-surface ( $R_{\text{NS}}, \theta_0$ ), a parametric equation describing the field line is given by:

$$\frac{\sin^2 \theta}{r} = \text{constant} \equiv \frac{\sin^2 \theta_0}{R_{\text{NS}}} . \quad (6)$$

Some straightforward calculations lead to an expression for the tangential angle  $\chi(x, \theta_0)$  of the  $\theta_0$ -field line:

$$\chi(x, \theta_0) = \Theta(x, \theta_0) + \arctan \left( \frac{1}{2} \tan \Theta(x, \theta_0) \right) . \quad (7)$$

Here  $x = r/R_{\text{NS}}$  and  $\Theta(x, \theta_0) = \arcsin(\sqrt{x} \cdot \sin \theta_0)$  is the radial angle of the  $\theta_0$ -field line at a distance  $x$  (see also Lyne & Graham-Smith 1990). The geometry is displayed in Fig. 1. This can be used to calculate the polar angle  $\theta_S$  for a given distance  $x$  at which a ray propagates, that was emitted tangentially from the  $\theta_0$ -field line at the emission height  $x_{\text{em}}$ :

$$\theta_S(x, \theta_0) = \chi(x_{\text{em}}, \theta_0) - \arcsin \left[ \frac{x_{\text{em}}}{x} \cdot \sin(\pi - \chi(x_{\text{em}}, \theta_0) + \Theta(x_{\text{em}}, \theta_0)) \right] . \quad (8)$$

Using this point  $(x, \theta_S)$ , the footpoint-angle  $\theta_{S0}$  of the corresponding field line can be calculated using Eq. (6).

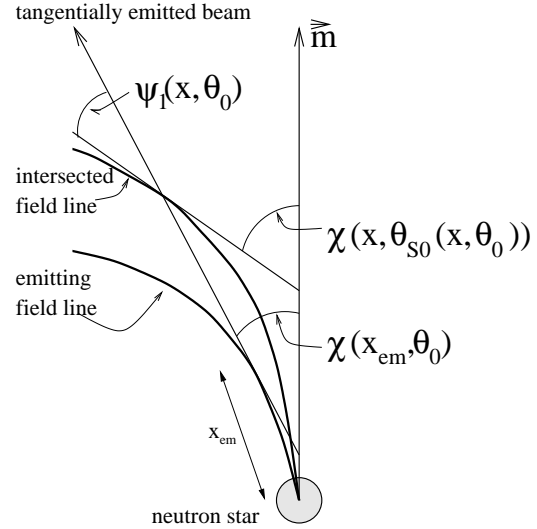


**Fig. 2.** Geometry to derive the intersecting angle  $\psi_1(x, \theta_0)$  between a beam which was emitted tangentially from the  $\theta_0$ -field line at the emission height  $x_{\text{em}}$  and a field line in a radial distance  $x$ .

The intersecting angle between a ray emitted tangentially from the  $\theta_0$  field line in the emission height  $x_{\text{em}}$  with the field line at the distance  $x$  can then be found as the difference of the tangential angles

$$\psi_1(x, \theta_0) = \chi(x, \theta_{S0}(x, \theta_0)) - \chi(x_{\text{em}}, \theta_0) , \quad (9)$$

as is shown in Fig. 2.

### 2.2.2. Other contributions

The rotation of the magnetosphere causes additional effects which have to be considered for the intersecting angle. The radiation is bent forward into the direction of rotation by *aberration*. Following Phillips (1992), the magnitude of this effect is

$$\theta_{\text{ab}}(x) = \arctan \left( 2\pi \frac{x R_{\text{NS}} \sin \alpha}{cP} \right) . \quad (10)$$

At larger distances from the NS, corotation of the plasma cannot be maintained, and *magnetic sweep-back* becomes important. The calculation of this effect is rather complex, but an approximation was given by Shitov (1983):

$$\theta_{\text{msb}}(x) \simeq 1.2 \cdot \left( \frac{2\pi x R_{\text{NS}}}{cP} \right)^3 \cdot \sin^2 \alpha . \quad (11)$$

The direction of this effect is backwards relative to the rotation. To calculate the net-effect of these two contributions, one has to take their difference at the distance  $x$  and subtract their value at the emission height  $x_{\text{em}}$ . It is therefore given by

$$\psi_2(x) = \theta_{\text{ab}}(x) - \theta_{\text{ab}}(x_{\text{em}}) - \theta_{\text{msb}}(x) + \theta_{\text{msb}}(x_{\text{em}}) . \quad (12)$$

Angular contributions by effects of general relativity are negligible at distances larger than a few km from the NS surface (e.g. Gonthier & Harding 1994). Since the contribution will always be much smaller than the accuracy of our calculations, which is restricted to the beaming angle of  $1/\gamma_{\text{beam}}$ .

### 2.2.3. Resultant intersection angle

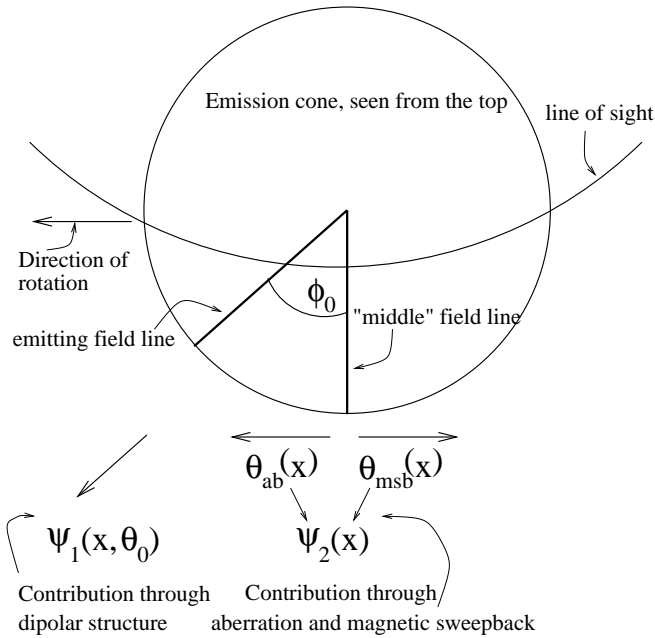


**Fig. 3.** Geometry to derive the resultant intersection angle under consideration of the dipolar contribution and those of aberration and magnetic sweep-back.  $\psi_1$  points towards the direction of the emitting field line,  $\theta_{\text{ab}}$  into the direction of rotation.  $\theta_{\text{msb}}$  points backwards relative to the direction of rotation.

For the resultant intersection angle (see Fig. 3), the curvature direction of the emitting field line has to be taken

into account. This can be defined as the angle between the plane of curvature of the emitting field line and the field line in the middle of the profile  $\phi_0$ . The tube of emitting field lines then rotates into the direction of the field line with  $\phi_0 = 90^\circ$ .

The resultant angle of a beam, radiated from the  $\theta_0$ -field line into the direction  $\phi_0$  at the emission height  $x_{\text{em}}$ , which intersects with a field line in a distance  $x$  from the NS can then be given as:

$$\psi_{\text{S}}(x, \theta_0) = [(\psi_1(x, \theta_0) \cos \phi_0)^2 + (\psi_2(x) - \psi_1(x, \theta_0) \sin \phi_0)^2]^{\frac{1}{2}} . \quad (13)$$

This equation is only valid if one regards the intersecting angle at a sufficient distance from the emitting altitude, where  $\psi_{\text{S}}$  reaches a finite value. At the emission region itself,  $\psi_{\text{S}}$  would be zero. As the radiation is beamed into a forward-cone of  $1/\gamma_{\text{beam}}$ , and the intersected field lines are all nearly parallel in the emission region, we use this beaming-angle  $\psi_{\text{S}} = 1/\gamma_{\text{beam}}$  for  $x \simeq x_{\text{em}}$ .

In Fig. 4, the intersection angle between a tangentially emitted beam and a field line at a given distance is displayed from the emission height to  $R_{\text{LC}}$  for a canonical pulsar.

### 2.2.4. The canonical pulsar

As we require a number of intrinsic pulsar parameters for our calculations, we use the mean values from the known pulsar sample. These parameters are  $P = 0.6$  s and  $\dot{P} = 10^{-14.6}$ . For the magnetic inclination we assume  $\alpha = 40^\circ$ . The regarded field line is at  $\phi_0 = 40^\circ$  and  $\theta_0 = \theta_{\text{lof}}/1.5$  ( $\theta_{\text{lof}}$  is the footpoint angle of the last open field line, see Eq. 2). As a typical emission height we choose 2% of  $R_{\text{LC}}$ , which corresponds to slightly more than 50 pulsar radii for the canonical pulsar. For the Lorentz factor of the background plasma we use  $\gamma_{\text{bg}} = 1.7$ , following Kunzl (1997). In those cases, where we derive properties at a given distance in the magnetosphere, we use a point at 20% of the light cylinder radius for  $R_{\text{LP}}$  (see also Sect. 3.1). As a typical value for  $\gamma_{\text{beam}}$  we assume a value of 50 (e.g. Rathnasree 1996, Kunzl 1997). As stated earlier, the value of  $\gamma_{\text{beam}}$  is only important very close to the emission region itself.

### 2.3. Approximation for the Dielectric Tensor

In order to derive the properties of the natural wave modes it is necessary to get an approximate idea of the dielectric characteristics of the plasma. Our approach follows the work of Melrose (1979), which is based on two assumptions:

- The plasma is in the *low density limit*, which is defined by the condition that the Alfvén velocity is much larger

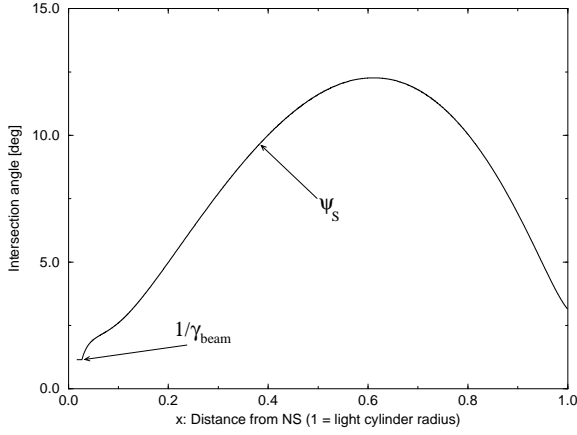


**Fig. 4.** Resultant intersection angle for a canonical pulsar (see text for assumed parameters). The angle is displayed from the emission height to the light cylinder radius.

than the velocity of light ( $v_A \gg c$ ). Combining the Alfvén velocity

$$v_A^2 = \frac{B^2}{\mu_0 \rho} \quad (14)$$

with the relativistic mass density  $\rho = \gamma_{\text{bg}} m_e \cdot n$  leads to the condition

$$\frac{B^2}{c^2 \cdot \mu_0 \gamma m_e n} \gg 1. \quad (15)$$

This condition is well fulfilled throughout the pulsar magnetosphere. For our calculations this implies that the dielectric tensor is close to unity.

- The background-plasma is assumed to be cold. This follows from the consideration that the coherent radiation mechanism can only be effective for particle energies above a certain threshold (see Eq. 5). The final particle energies will therefore peak at this critical value.

Thus the *long wavelength approximation* applies, which can be used when the wavelength of the propagating wave is much larger than the relevant lengths in the plasma. This approximation should be fulfilled throughout in the pulsar magnetosphere above the emitting region.

Using the low density limit the dielectric tensor may be written as

$$\epsilon_{ij} = \delta_{ij} + \Delta\epsilon_{ij} \quad (16)$$

with  $\Delta\epsilon_{ij} \ll 1$ . The dispersion equation is then found as

$$An^4 - Bn^2 + C = 0 \quad (17)$$

with  $A, B$  and  $C$  being functions of  $\epsilon_{ij}$ . In this approximation  $\Delta\epsilon_{ij}$  does not depend on  $n$ . Hence two solutions can be given for  $n^2$  (Melrose & Stoneham 1977):

$$n^2 = 1 \pm \Delta n_{\pm}^2 \quad (18)$$

$$\Delta n_{\pm}^2 = \frac{a + b \pm \sqrt{(a-b)^2 + 4g^2}}{2}. \quad (19)$$

Using the cold plasma approximation for electrons the dielectric tensor leads to

$$a = -\frac{\omega_{\text{pe}}^2 (\cos \theta - \beta)^2}{\omega^2 (1 - \beta \cos \theta)^2 - \Omega_e^2} - \frac{\omega_{\text{pe}}^2 \sin^2 \theta}{\gamma_{\text{bg}}^2 \omega^2 (1 - \beta \cos \theta)^2} \quad (20)$$

$$b = -\frac{\omega_{\text{pe}}^2 (1 - \beta \cos \theta)^2}{\omega^2 (1 - \beta \cos \theta)^2 - \Omega_e^2} \quad (21)$$

$$g = \frac{\omega_{\text{pe}}^2 (\Omega_e / \omega) (\cos \theta - \beta)}{\omega^2 (1 - \beta \cos \theta)^2 - \Omega_e^2}, \quad (22)$$

$\beta = v/c$ . The electron plasma frequency  $\omega_{\text{pe}}$  and the electron gyro frequency  $\Omega_e$  are defined as:

$$\omega_{\text{pe}} \equiv \sqrt{\frac{n \cdot e^2}{\gamma m_e \epsilon_0}} \quad (23)$$

$$\Omega_e \equiv \frac{|e| \cdot B}{\gamma m_e}. \quad (24)$$

$n$  is the plasma density ( $n(x) = n_{\text{GJ}}/x^3$ , see Eq. 3),  $e$  the elementary charge,  $m_e$  the electron mass and  $\epsilon_0$  the electric field constant.  $B$  is the magnetic field strength ( $B(x) = B_0/x^3$ , see Eq. 4).

With these parameters, the axial ratio of the polarization ellipses of the two natural wave modes can be calculated:

$$T_{\pm} = \frac{2g}{a - b \mp \sqrt{(a-b)^2 + 4g^2}}. \quad (25)$$

$T = 0$  and  $T = \pm\infty$  correspond to linear polarizations. For elliptical polarizations  $T$  becomes finite. The rotating sense of a positive  $T$  is right hand with respect to the direction of propagation and left hand for negative  $T$ .

The degree of circular polarization can then be calculated through

$$\Pi_{V\pm} := \sin(2 \arctan T_{\pm}). \quad (26)$$

As a natural wave mode is fully polarized per definition, the linear polarization can be calculated as the quadratic complement:

$$\Pi_{L\pm} := \sqrt{1 - \Pi_{V\pm}^2}. \quad (27)$$

### 3. Results

The polarization of the natural wave modes depends mainly on the angle between the propagating electromagnetic wave and the magnetic field. If the wave propagates purely parallel to the field ( $\mathbf{k} \parallel \mathbf{B}$ ,  $\mathbf{k}$  being the wave vector of the propagating beam), the modes obviously have to be circularly polarized since no linear direction perpendicular to  $\mathbf{k}$  is preferred. When  $\mathbf{k}$  is perpendicular to  $\mathbf{B}$ , a direction is preferred and the wave is fully linearly polarized. If the angle between  $\mathbf{k}$  and  $\mathbf{B}$  becomes larger than  $90^\circ$  then the handedness of the circular polarization gets reversed

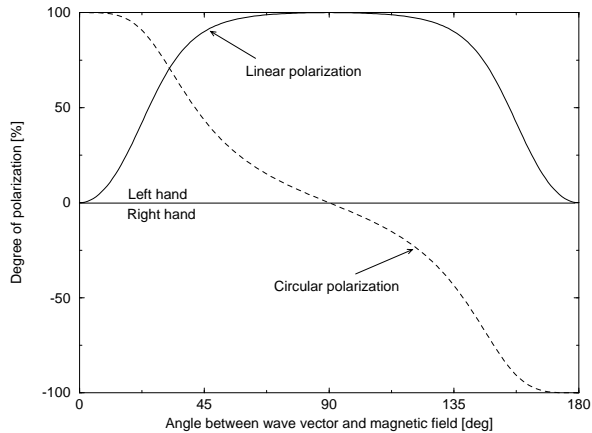


**Fig. 5.** Degree of polarization of one natural wave mode versus the intersecting angle between the propagating wave and the magnetic field. In this figure we show the principal polarization behaviour of one natural mode of a wave propagating at an oblique angle to the magnetic field through a non relativistic ( $\gamma_{bg} = 1$ ) cold electron plasma. The function was calculated for a frequency of 1 GHz and a magnetic field strength of 0.2 T. For small angles between  $k$  and  $B$  the polarization is mainly circular, as no linear direction is preferred perpendicular to  $k$ . At an angle close to  $90^\circ$  the polarization is mainly linear, for angles larger than  $90^\circ$  it becomes increasingly circular again but with an reversed handedness (due to the opposite direction of gyration). The transition between fully circular to fully linear depends heavily on the frequency and the magnetic field strength. For plasma Lorentz factors  $\gamma_{bg} > 1$ , the angle gets Lorentz transformed – thus shifting the condition for transverse propagation to smaller angles.

for each mode due to the opposite direction of the particle gyration.

The transition (for an example see Fig. 5) between these two states depends strongly on a number of parameters:

- The magnetic field strength. For a strong magnetic field, the transition from circular to linear polarization occurs for very small angles between  $k$  and  $B$ .
- The frequency. For lower frequencies, a higher degree of linear polarization is reached at smaller angles than for higher frequencies.
- The plasma  $\gamma$ -factor. For a relativistic plasma, the intersecting angle between the propagating beam and the magnetic field is Lorentz-transformed, such that the angle increases. The transverse propagation ( $\sim 90^\circ$  in Fig. 5) is reached at a smaller angle.

### 3.1. Qualitative polarization characteristics

We apply these calculations to the propagation of an electromagnetic wave through the pulsar magnetosphere using canonical pulsar parameters (Sect. 2.2.4) and taking into account all angular effects.

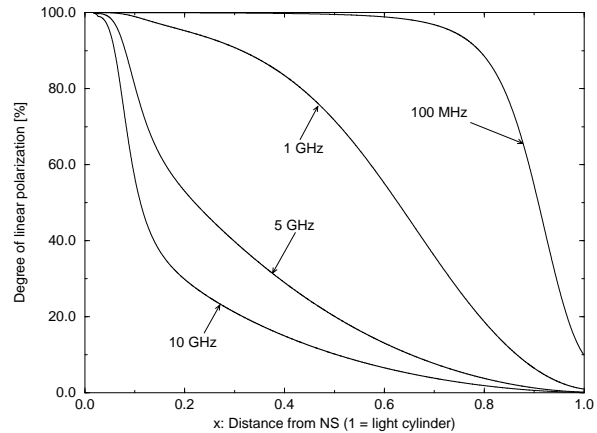


**Fig. 6.** Degree of linear polarization of one natural wave mode versus the distance from the NS (up to the light cylinder radius) for the canonical pulsar (Sect. 2.2.4).

Figure 6 illustrates the change of the natural wave mode polarization characteristics with distance from the pulsar for different frequencies. For clarity, we displayed only the linear polarization for one mode (the + mode, see Eq. 18). As the circular polarization is given by the quadratic complement (see Eq. 27), a decrease of the linear polarization leads to an increase of the circular contribution. The dominating parameter is the rapidly decreasing magnetic field. After the radiation, the kinetic energy of the plasma is relatively low. Following Kunzl (1997), we use a background Lorentz factor of  $\gamma_{bg} = 1.7$ . This value would result from a free electron maser emission mechanism through comparing bunching- and loss times. Other radiation mechanisms lead to different values of  $\gamma_{bg}$  but the qualitative manner does not change. The dependence on  $\gamma_{bg}$  is discussed separately in Sect. 3.2.3.

The following qualitative behaviour can be observed. Close to the emitting region, the mode is fully linearly polarized for all frequencies due to the extremely high magnetic field in the emitting region ( $|B| \simeq 10^3$  T). As the wave propagates outwards, the intersecting angle increases and the magnetic field decreases. Initially this just causes the linear polarization of the high frequency waves to decrease, while the lower frequency waves maintain a high degree of linear polarization up to a large distance from the NS. Thus, if only one mode is observed at a time, for a given distance we expect a *decrease* of linear polarization with frequency and an *increase* of circular polarization.

As stated earlier, it remains unclear up to which distance from the NS the polarization of the propagating radiation is influenced by the changes of the natural wave modes ( $R_{LP}$ ). This remains to be a problem to be solved by mode coupling theory but appears to be rather complicated as the plasma is most likely highly inhomogeneous in space and time. Therefore for the present discussion we choose an arbitrary distance for  $R_{LP}$  and derive the qualitative behaviour without loss of generality.

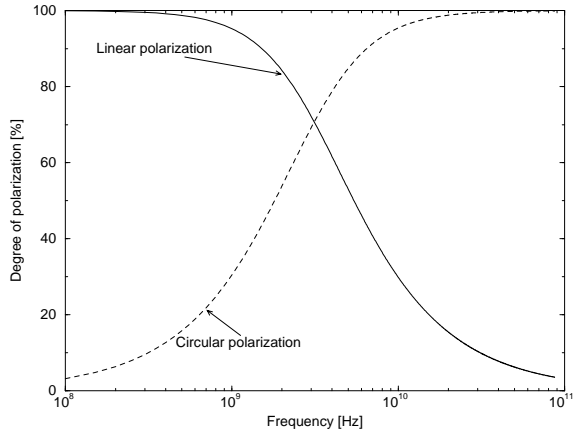


**Fig. 7.** Degree of polarization of one natural wave mode versus frequency. The height above the NS was chosen to be 20% of the light cylinder without loss of generality. The qualitative behaviour is a decrease of linear and an increase of circular polarization with frequency for the canonical pulsar (Sect. 2.2.4).

Figure 7 shows the frequency development of one natural wave mode at an arbitrary distance of 20% of  $R_{LC}$  for a typical pulsar. The degree of linear polarization should decrease and the degree of circular should increase above about one GHz.

### 3.2. Dependence on various pulsar parameters

We now want to investigate, how the change of polarization characteristics with frequency depends on the variation of other pulsar parameters.

#### 3.2.1. Spin-down luminosity

As stated in Sect. 1, a correlation between the degree of polarization and the spin-down luminosity  $\dot{E}$  has been observed at high frequencies.

$$\dot{E} = 4\pi^2 \cdot I \frac{\dot{P}}{P^3}, \quad (28)$$

$I$  is the moment of inertia. In order to perform our calculations for different values of  $\dot{E}$ , we keep all parameters fixed and change only the time derivative of the period  $\dot{P}$ . As before, the period was set to 0.6 s and for  $\dot{P}$  we used the values  $10^{-16.3}$ ,  $10^{-14.6}$  and  $10^{-12.1}$ . This corresponds to  $\dot{E}$  values of  $9 \cdot 10^{23}$  W,  $5 \cdot 10^{25}$  W and  $1 \cdot 10^{28}$  W respectively

Figure 8 shows that for high  $\dot{E}$  pulsars the degree of linear polarization decreases at a higher frequency than for low  $\dot{E}$  pulsars. This is in agreement with the observations, especially if one follows the argument of Sect. 2.1 and takes the degree of polarization as an upper limit. At low frequencies, all pulsars have a high degree of linear polarization as an upper limit. Therefore no correlation with  $\dot{E}$  is expected. At higher frequencies – in contrary –

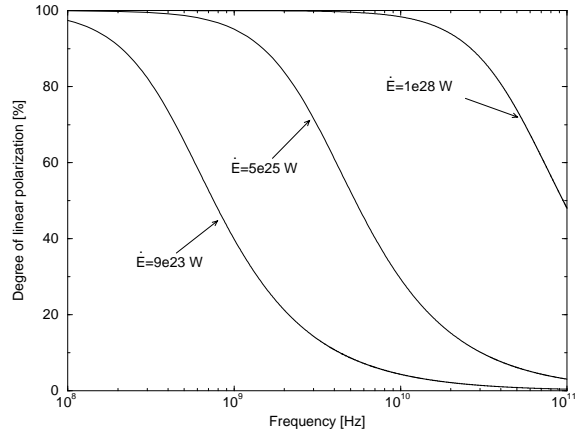


**Fig. 8.** Degree of linear polarization of one natural wave mode versus frequency for different spin down luminosities  $\dot{E}$ . We used the same canonical pulsar parameters as before except that we varied the values for  $\dot{P}$ , keeping the period fixed at  $P = 0.6$  s. The resulting values for  $\dot{E}$  are written next to the curves. For pulsars with a higher  $\dot{E}$  the decrease in linear polarization occurs at a higher frequency.

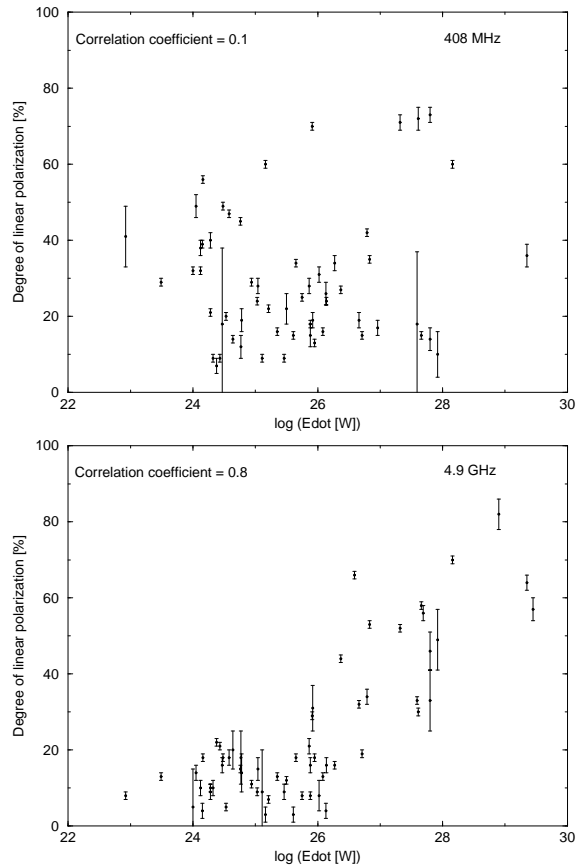


**Fig. 9.** Measured degree of linear polarization versus the spin down luminosity  $\dot{E}$  at 408 MHz (upper plot) from Gould & Lyne (1998) and 4.9 GHz (lower plot), taken with the 100 m Effelsberg radio telescope. The two plots consist of (nearly) the same set of pulsars. These observations correspond to the predictions of Fig. 8. At the higher frequency, pulsars with a low  $\dot{E}$  have a low degree of linear polarization. At low frequencies no such correlation can be observed which again corresponds to Fig. 8. At low frequencies the degree of linear polarization is nearly independent of  $\dot{E}$ .



the upper limit for low- $\dot{E}$  pulsars is low, whereas high- $\dot{E}$  pulsars can still exhibit highly linearly polarized radio emission. A correlation is therefore expected at those frequencies.

### 3.2.2. Period

The next parameter we vary is the period. In the list of observational constraints in Sect. 1 it was stated that only for short-period pulsars highly linearly polarized high frequency radio emission has been observed. We therefore keep all parameters fixed and vary only the period. The emission height was set to 2 % of the light cylinder radius (and therefore changes in absolute numbers as the light cylinder radius varies with the period).

Figure 10 shows that short-period pulsars can maintain a higher degree of linear polarization up to a higher frequency than long-period pulsars. This is in excellent agreement with the observations. At low frequencies the linear polarization can be high for all periods, we therefore would not expect an observable correlation. At high frequencies in contrast we therefore *do* expect an inverse correlation.

### 3.2.3. Lorentz-factor of the background plasma

The Lorentz-factor of the background plasma is important because the intersecting angle gets Lorentz transformed. If one increases the Lorentz factor at a given point, the Lorentz-transformed intersection angle first increases up to  $90^\circ$  in the plasma frame, resulting in fully linearly polarized modes of transverse propagation (see Fig. 5). A further increase of  $\gamma_{\text{bg}}$  leads to angles  $> 90^\circ$ . The degree of linear polarization then decreases again and the circular contribution changes its handedness. This behaviour can be seen in Fig. 12. One consequence is that if the Lorentz transformed intersecting angle between the propagating wave and the magnetic field is close to perpendicular, small, local variations in the conditions can result into changes in the handedness of the circular polarization. As we have to assume that the plasma conditions are highly inhomogeneous in space and time, this effect could well account for sudden changes in handedness observed in low degree circular polarizations.

An inference which can be made is that the background Lorentz factor cannot be very large, e.g. larger than a few hundred.

### 3.3. Refractive indices

So far we only regarded the polarimetric properties of *one* natural wave mode. But, as mentioned in Sect. 1, observations suggest that both modes are present in the pulsar radio emission as the familiar OPMs. They can be observed both separated (leading to highly polarized parts in the pulse profile with a smooth variation of the PPA)

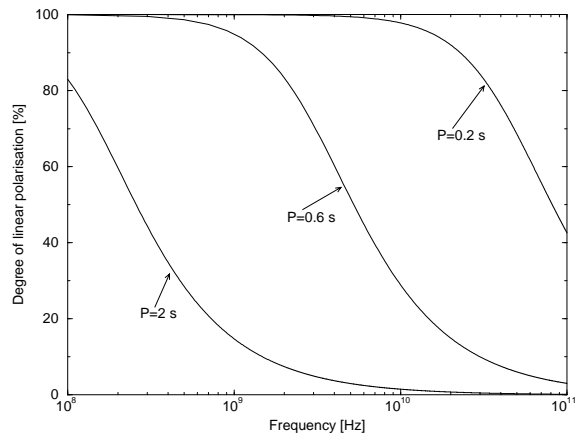


**Fig. 10.** Degree of linear polarization of one natural wave mode versus frequency for different pulsar periods.  $\dot{P}$  was held fixed at  $10^{-14.6}$ , the emission height at 2% and  $R_{\text{LP}}$  at 20 % of  $R_{\text{LC}}$ . Short-period pulsars can maintain a higher degree of polarization up to a higher frequency than their long-period counterparts.

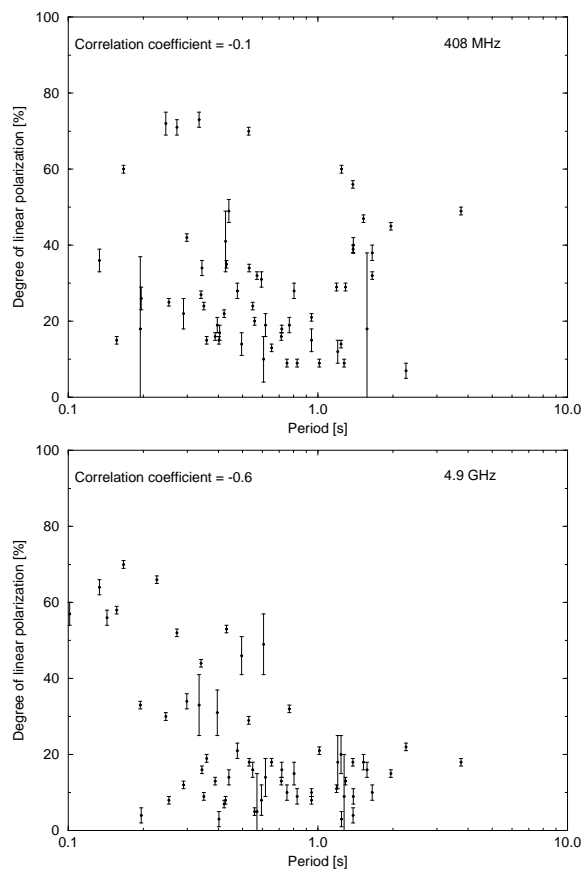


**Fig. 11.** Measured degree of linear polarization versus period at 408 MHz (upper plot) from Gould & Lyne (1998) and 4.9 GHz (lower plot), taken with the 100 m Effelsberg radio telescope. The two plots consist of (nearly) the same set of pulsars. These observations correspond to the predictions of Fig. 10. At the higher frequency, pulsars with a long period radiate with a low degree of linear polarization. At low frequencies no such correlation can be observed which again corresponds to Fig. 10. At low frequencies the degree of linear polarization is nearly independent of the period.

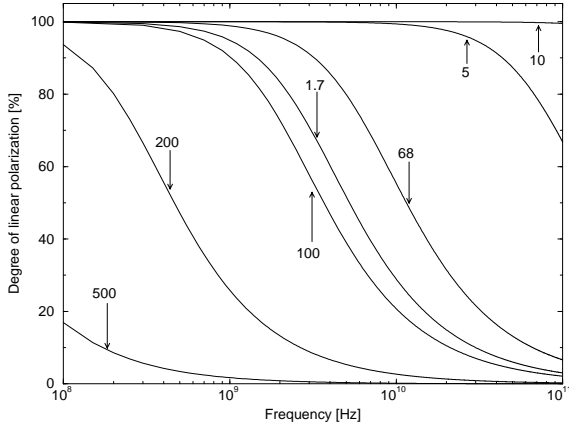


**Fig. 12.** Degree of linear polarization of one natural wave mode versus frequency for different background Lorentz-factors (the values are written next to the curves). As the intersecting angle between the propagating wave and the magnetic field is Lorentz transformed, the degree of linear polarization first increases with  $\gamma_{bg}$  until the transformed angle reaches  $90^\circ$  and then decreases again for larger resulting angles. The difference is the handedness of the circular contribution for high and low  $\gamma_{bg}$  factors.

and superposed (leading to weakly polarized parts of the profile with often erratic variations in the PPA).

A spatial separation of polarized modes in a medium is caused by birefringence, where both modes propagate independently with different indices of refraction (a familiar example for such a medium is the calcite crystal). Different indices of refraction lead to an angular separation which may result into an independent observation of the two modes. The magnitude of this angular separation is given by

$$\xi_{\text{refr}} = \frac{\delta(n_+ - n_-)}{\delta\psi_S} \quad (29)$$

(Melrose 1979). Clearly the separation depends on the difference between the two indices of refraction. The larger the difference is, the better is the chance, that we observe the two modes separately. If the difference is small, we expect increasing superposition of the two modes, thus leading to a depolarization.

Figure 13 shows the frequency dependence of the refractive indices of the two natural wave modes. The deviations of the indices from unity are displayed:  $n_{\pm}^2 = 1 + \Delta n_{\pm}^2$  (see Eq. 18). The +mode corresponds to the X-mode (the polarization vector lies in the plane spanned by  $\mathbf{k}$  and  $\mathbf{B}$ ), the -mode to the O-mode (polarization vector perpendicular to  $\mathbf{k}$  and  $\mathbf{B}$ ).

Two conclusions can be drawn from the diagram: **1.** The refractive index of the O-mode is much stronger influenced by propagation effects than the one of the X-mode. This corresponds to the result of Barnard & Arons (1986), that the X-mode can propagate through the magnetosphere nearly undisturbed, whereas the O-mode is tight

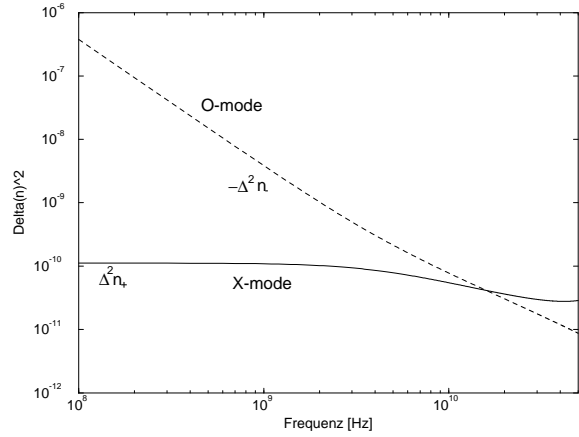


**Fig. 13.** Deviations of the two squared indices of refraction of the natural wave modes from unity ( $n^2 = 1 + \Delta n_{\pm}^2$ ). Note that  $\Delta n_-^2$  is negative.  $\Delta n_+^2$  (solid line) belongs to the refractive index of the X-mode and  $\Delta n_-^2$  (dashed line) to the one of the O-mode. The assumed parameters are those of the canonical pulsar defined in Sect. 2.2.4. For the O-mode, the magnitude of  $\Delta n^2$  is much larger and the frequency dependence is much stronger than for the X-mode. The difference between the two refractive indices clearly decreases with increasing frequency.

to the bending of the field lines. **2.** The difference between the two refractive indices decreases with increasing frequency. This may lead to increasing superposition of the two natural wave modes (either intrinsically or through the limited spatial and temporal resolution of the observation). If the phases of the modes are uncorrelated, this will cause a depolarization of the observed polarization.

If this conclusion is correct – depolarization at higher frequencies through superposition of OPMs – an additional depolarization envelope is superposed on our previous discussion. This depolarization could be responsible for the low number of pulsars which show the increasing degree of circular polarization towards high frequencies.

The difference between the two indices depends on other pulsar parameters as well. Figure 14 displays the frequency dependence of this difference for various values for  $\dot{E}$ .  $n_+ - n_-$  is larger for larger values of  $\dot{E}$ . This leads to a depolarization at higher frequencies compared to pulsars with a low  $\dot{E}$ . The peak in the curve for  $\dot{E} = 5 \cdot 10^{25}$  W is caused by a resonance when the wave reaches the Doppler shifted gyro frequency. It is questionable whether the made approximation is valid at this particular point. Following Melrose (1979) and Beskin et al. (1993) we therefore neglect the resonance and join the asymptotic course on both sides of the peak.

## 4. Conclusions

We have used the approximation of the dielectric tensor for the low frequency limit to derive the general properties of the natural wave modes in the radio pulsar magnetosphere. The approximation of the dielectric tensor in the

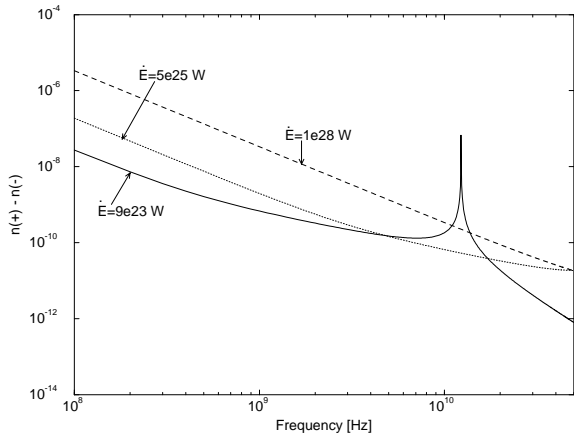


**Fig. 14.** The difference between the refractive indices of the two natural wave modes  $n_+ - n_-$  versus frequency for different values of  $\dot{E}$ . The difference is larger for pulsars with a high  $\dot{E}$  which should therefore suffer depolarization effects at higher frequencies than low  $\dot{E}$ -pulsars. The peak in the curve for  $\dot{E} = 5 \cdot 10^{25}$  W is caused by a resonance when the wave hits the Doppler shifted gyro frequency and should therefore be neglected (see text).

given limit implies that the plasma is sufficiently cold. Following Melrose (1979) this should be true for pulsar magnetospheres.

Electromagnetic waves, which propagate through a plasma at an oblique angle to the magnetic field, adopt two orthogonal natural wave modes with individual indices of refraction. We identify these modes with the familiar orthogonal polarization modes. It was our aim to derive the polarimetric properties of these modes and calculate their dependence on different parameters under special consideration of the various angles involved.

We regard only one natural mode assuming that we see only one mode at a time. This assumption is of course not always true, but the existence of highly polarized emission in single pulses indicates that at least sometimes it is true. If both modes are recorded simultaneously, it will lead to a depolarization of the observed radiation. Our results can therefore be regarded as upper limits for the observed degree of polarization. In the case of a highly linearly polarized natural mode we cannot predict the degree of linear polarization one will observe. But if the mode has only a low level of linear polarization, a low level for the observed radiation is predicted.

The main uncertainty of our calculations is the radius of limiting polarization ( $R_{LP}$ ). However, as we are mainly interested in the qualitative behaviour of the polarization, we have used a fixed value for  $R_{LP}$  without restriction of generality. For a different value of  $R_{LP}$  the numbers may change but the general behaviour remains. This is even true if one moves  $R_{LP}$  to its possible extremes: the light cylinder radius and just above the emission region.

Our results are in excellent agreement with the observations: **1.** The degree of linear polarization decreases towards high frequencies (Fig. 7). The decrease in linear polarization implies an increase in circular polarization (within this concept). This is in agreement with recent observations which show the existence of some pulsars which have this peculiar polarimetric property (von Hoensbroech et al. 1998). **2.** Given a set of specific pulsar parameters, a variation of  $\dot{P}$  leads to a variation in the spin down luminosity  $\dot{E}$ . Figure 8 shows that the degree of linear polarization of pulsars with a high  $\dot{E}$  decreases at higher frequencies than for pulsars with a lower  $\dot{E}$ . Thus a correlation between the polarization at high frequencies and  $\dot{E}$  should exist. Such a correlation has been indeed observed. **3.** Similar to the above point, we have varied the period, keeping all other pulsar parameters fixed (Fig. 10). The degree of linear polarization for long period pulsars is expected to decrease at lower frequencies than for short periods pulsars. This should give an inverse correlation between the degree of linear polarization at high frequencies and the period. Again, such an inverse correlation has been observed at a frequency of 5 GHz.

No investigation could be made for the change of the polarimetric characteristics along the different field lines, which are observed during a pulse. The reason is that the qualitative change depends heavily on  $R_{LP}$ . For future work it therefore seems to be important to find an estimate for this distance.

The difference between the refractive indices of the two modes decreases with frequency. As this implies a closer propagation of the modes, we expect an increasing superposition. This would lead to a depolarization of the observed radiation at high frequencies. Such a depolarization could account for low abundance of pulsars which show an increasing degree of circular polarization with frequencies.

We note again that our calculations are based on the two assumptions that the background plasma is cold and is dominated by particles with one sign of charge. The obvious advantage of these assumptions – negligible spread of the energy distribution and no strong pair production – is their physical and mathematical simplicity. The more it is astounding that we can qualitatively reproduce the complex properties of pulsar radio polarization. In general both assumptions are not widely accepted. Either the energy distribution of the plasma is usually taken to be extended (Arons & Barnard 1986; Lyutikov 1998 and references therein) or the secondarily produced electron and positron pairs are expected to dominate the particle content of the pulsar magnetosphere (e.g. Sturrock 1971, Cheng & Ruderman 1977 and Daugherty & Harding 1982). However the expressiveness of our model deserves further considerations.

*Acknowledgements.* We want to thank R. Wielebinski, R.T. Gangadhara, M. Kramer, A. Jessner, D.R. Lorimer and K.M. Xilouris for helpful discussions and support of this work. We

also thank the anonymous referee for helpful comments on the manuscript.

## References

- Allen C.A., Melrose D.B., 1982, Proc. ASA 4, 365  
 Arons J., Barnard J.J., 1986, ApJ 302, 120  
 Barnard J.J., 1986, ApJ 303, 280  
 Barnard J.J., Arons J., 1986, ApJ 302, 138  
 Beskin V.S., Gurevich A.V., Istomin Y.N., 1993, Physics of the Pulsar Magnetosphere, Cambridge University Press  
 Blaskiewicz M., Cordes J.M., Wasserman I., 1991, ApJ 370, 643  
 Cheng A.F., Ruderman M.A., 1977, ApJ 214, 598  
 Cheng A.F., Ruderman M.A., 1979, ApJ 229, 348  
 Cocke J.W., Pacholczyk A.G., 1976, ApJ 204, L13  
 Cordes J.M., Hankins T.H., 1977, ApJ 218, 484  
 Cordes J.M., 1978, ApJ 222, 1006  
 Daugherty J.K., Harding A.K., 1982, ApJ 252, 337  
 Gangadhara R.T., 1997, A&A 327, 155  
 Gil J., 1991, A&A 243, 219  
 Gil J., Kijak J., 1997, MNRAS 288, 631  
 Goldreich P., Julian W.H., 1969, ApJ 157, 869  
 Gonthier P.L., Harding A.K., 1994, ApJ 425, 767  
 Gould D.M., Lyne A.G., 1998, MNRAS submitted  
 Harding A.K., Tademaru E., 1979, ApJ 233, 317  
 Harding A.K., Tademaru E., 1980, ApJ 238, 1054  
 Harding A.K., Tademaru E., 1981, ApJ 243, 597  
 von Hoensbroech A., Xilouris K.M., 1997, A&A 324, 981  
 von Hoensbroech A., Kijak J., Krawczyk A., 1998, A&A in press  
 Krall N.A., Trivelpiece A.W., 1986, Principles of Plasma Physics, San Francisco Press  
 Kramer M., Xilouris K.M., Jessner A. et al., 1997, A&A 322, 846  
 Kunzl T., 1997, Diploma Thesis, University of Munich  
 Lange C., Kramer M., Wielebinski R., Jessner A., 1998, A&A in press  
 Lyne A.G., Graham-Smith F., 1990, Pulsar Astronomy, Cambridge University Press  
 Lyutikov M., 1998, MNRAS 293, 447  
 Manchester R.N., 1971, ApJS 23, 283  
 Manchester R.N., Taylor J.H., 1977, Pulsars, Freeman, San Francisco  
 Manchester R.N., Taylor J.H., Huguenin G.R., 1975, ApJ 196, 83  
 McKinnon M.M., 1997, ApJ 475, 763  
 Melrose D.B., 1979, Proc. ASA 3, 120  
 Melrose D.B., Stoneham R.J., 1977, Proc. ASA 3, 120  
 Morris D., Graham A.D., Sieber W., 1981, A&A 100, 107  
 Phillips J.A., 1992, ApJ 385, 282  
 Radhakrishnan V., Cooke D.J., 1969, Astrophys. Lett. 3, 225  
 Radhakrishnan V., Rankin J.M., 1990, ApJ 352, 258  
 Rankin J.M., 1990, ApJ 352, 247  
 Rathnasree N., 1996, in Johnston S., Walker M.A., Bailes M., eds, IAU Colloq. 160, Pulsars: Problems and Progress, ASP Conf. Series, Vol. 105, p. 221  
 Shitov Y.P., 1983, Sov. Astron. 27, 314  
 Stinebring D.R., Cordes J.M., Rankin J.M., Weisberg J.M., Boriakoff W., 1984, ApJS 55, 247  
 Sturrock P.A., 1971, ApJ 164, 529  
 Thorsett S.E., 1991, ApJ, 377, 263  
 Xilouris K.M., Seiradakis J.H., Gil J., Sieber W., Wielebinski R., 1995, A&A 293, 153  
 Xilouris K.M., Kramer M., Jessner A., Wielebinski R., Timofeev M., 1996, A&A 309, 481

